Adsorbed states of NH_3 and C_6H_6 on the Si(111)$(\sqrt{3}\times\sqrt{3})R30°$-B surface: Thermal-desorption and electron-energy-loss-spectroscopy studies

Y. Taguchi*
College of Engineering, University of Osaka Prefecture, Gakuen-cho 1, Sakai, Osaka 593, Japan

M. Daté, N. Takagi, T. Aruga, and M. Nishijima
Department of Chemistry, Faculty of Science, Kyoto University, Kyoto 606-01, Japan
(Received 29 July 1994)

Adsorbed states of NH_3 and C_6H_6 on a Si(111)$(\sqrt{3}\times\sqrt{3})R30°$-B surface have been studied by the use of thermal desorption and high-resolution electron-energy-loss spectroscopy. At 90 K, a bulklike NH_3 multilayer, NH_3 hydrogen bonded to a chemisorbed one, and molecularly chemisorbed NH_3 exist on the $(\sqrt{3}\times\sqrt{3})R30°$-B surface. These desorb at $\sim$115, 140, and 170 K, respectively. Chemisorbed NH_3 has a very low NH stretching energy of $\sim$370 meV, and its N-H bonds are significantly weakened. A 2.0-eV loss, which corresponds to the electronic transition from an occupied backbond state to an empty dangling-bond state of the Si adatom on the $(\sqrt{3}\times\sqrt{3})R30°$-B surface, is removed upon NH_3 adsorption. It is proposed that chemisorbed NH_3 is coordinated to the Si adatom on the surface. C_6H_6 does not chemisorb on the $(\sqrt{3}\times\sqrt{3})R30°$-B surface even at 90 K, but only physisorbs at <160 K. The adsorbed states of NH_3 and C_6H_6 on the $(\sqrt{3}\times\sqrt{3})R30°$-B surface are quite different from those on clean Si surfaces, and the reactivity criterion of the surface is discussed. It is also found that the $(\sqrt{3}\times\sqrt{3})R30°$-B surface has few defects when a large number of B atoms ($\sim 7\times10^{19}$ cm^{-3}) exists in the subsurface, which was evaluated by analyzing the surface-plasmon loss.

I. INTRODUCTION

Recent measurements have demonstrated that a $(\sqrt{3}\times\sqrt{3})R30°$-B superstructure is formed on Si(111) by the high-temperature heat treatment of a heavily B-doped Si wafer,[1] or by an adsorption of decaborane (DB), $B_{10}H_{14}$, followed by the thermal decomposition.[2] It has been found that the Si(111)$(\sqrt{3}\times\sqrt{3})R30°$-B surface has Si adatoms at the topmost layer (T_4 sites) and B atoms at the subsurface substitutional (S_5) sites directly beneath the adatoms, and that the Si adatom has an empty dangling-bond level due to a charge transfer from the adatom to the B atom beneath the adatom.[2–4] The chemical reactivity of Si modified by B atoms is of considerable interest, and the interactions of the $(\sqrt{3}\times\sqrt{3})R30°$-B surface with hydrogen atom,[5] oxygen,[6] and ammonia[2,7] have been studied. It has been found that the $(\sqrt{3}\times\sqrt{3})R30°$-B surface has chemical reactivities towards gas molecules quite different from those of clean Si surfaces.

We have investigated gas adsorption on clean Si surfaces for several years. For example, ammonia chemisorbs dissociatively on both Si(111)(7×7) and Si(100)(2×1) surfaces by forming the $SiNH_2$ and SiH surface species at 300 K.[8,9] On the other hand, the adsorbed state of benzene shows a distinct crystal-face specificity, and we have proposed that molecularly chemisorbed benzene is π bonded to the Si(111)(7×7) surface at $\leq$300 K,[10] and di-σ bonded to two adjacent Si atoms on the Si(100)(2×1) surface at <500 K.[11] In this work, we have studied the interactions of the Si(111)$(\sqrt{3}\times\sqrt{3})R30°$-B surface with NH_3 and C_6H_6 at 90–300 K by using thermal-desorption spectroscopy (TDS) and high-resolution electron-energy-loss spectroscopy (EELS). The $(\sqrt{3}\times\sqrt{3})R30°$-B surface was formed by heating Si(111) preexposed to DB.

By the use of photoemission spectroscopy, Avouris *et al.*[2] have proposed that there exists ammonia coordinated to the Si adatom on the Si(111)$(\sqrt{3}\times\sqrt{3})R30°$-B surface at 90 K. A preliminary EELS study was carried out by Yates[7] for the NH_3-exposed $(\sqrt{3}\times\sqrt{3})R30°$-B surface. However, the discussion was not given in detail and an evidence for NH_3 coordinated to the surface was not shown in the latter study. We have found vibrational and electronic transitions, which indicate the existence of NH_3 coordinated to the Si adatom on the $(\sqrt{3}\times\sqrt{3})R30°$-B surface at 90 K. C_6H_6 does not chemisorb on the $(\sqrt{3}\times\sqrt{3})R30°$-B surface, but only physisorbs on the surface at <160 K. By comparing the interactions of the $(\sqrt{3}\times\sqrt{3})R30°$-B surface with NH_3 and C_6H_6, the reactivity criterion of the surface has been proposed by both absolute electronegativity[12] of the molecule and the nature of the orbitals that interact with the surface.

In this work, we also examined the $(\sqrt{3}\times\sqrt{3})R30°$-B surface by EELS. The EEL spectra of the surface have been analyzed with the aid of the dipole scattering theory,[13–15] and the information on free carriers, which were introduced in the near-surface region by the high-temperature heat treatment in preparing the surface, was obtained: The concentration and Drude relaxation time of carriers in the near-surface region were estimated by the analysis of the surface-plasmon-loss profile, and the total number per unit area by that of the quasielastic peak.

II. EXPERIMENTAL

The experiments were performed by the *in situ* combined techniques of TDS, EELS, Auger electron spectroscopy (AES), and low-energy electron diffraction (LEED), by using an ultrahigh vacuum system with the base pressure of 1×10^{-8} Pa. The experimental apparatus used in the present study has been described elsewhere.[11] For specular-mode EELS measurements, an electron incidence angle θ_i of 65° with respect to the surface normal was used. The off-specular measurements were performed by rotating the monochromator around an axis, which was perpendicular to the incidence plane of electron beam. Electrons were scattered along the $[2\bar{1}\,\bar{1}]$ azimuth. All EEL spectra were measured at 90 K. The heating rate of 2.5 K/s was used for TDS measurements. The sample used ($7\times8\times0.5$ mm^3) was a Si(111) wafer of p-type, B doped, and 3000 Ω cm (B concentration: $<10^{13}$ cm^{-3}). The clean Si(111) surface, showing a sharp (7×7) LEED pattern, was prepared by several cycles of Ar^+-ion bombardment (450 eV, 10–20 μA cm^{-2}, 30 min) and annealing (1100 K for 2 min). No impurities were observed on the surface thus prepared within the detection limit of AES and EELS. Research-grade NH_3 (99.99% purity) and C_6H_6 (99.0 mol % purity) were used. DB (99% purity, SIGMA Chemical Company, U.S.A.) was used as a source of B, and the sample was exposed to DB after vaporization. DB and C_6H_6 were purified by freeze-pump-thaw cycles and were checked for the purities with a mass spectrometer. The DB, NH_3, and C_6H_6 gases were introduced into the vacuum chamber via an 8-mm-diam gas doser located 10 mm from the sample surface. The gas pressure was monitored by the use of a nude-type Bayard-Alpert ion gauge, and calibrated by the ion-gauge sensitivity factor relative to N_2: 0.6 for NH_3, 5.2 for C_6H_6, and 7.2 for DB estimated by referring to that of C_8H_{16}, which has the same number of electrons in one molecule. Exposures are given below in langmuir (1 L$=1.33\times10^{-4}$ Pa s).

III. RESULTS AND DISCUSSION

A. Si(111)$(\sqrt{3}\times\sqrt{3})R$30°-B

We have formed the Si(111)$(\sqrt{3}\times\sqrt{3})R$30°-B surface by exposing Si(111) to DB at 300 K and subsequently heating the sample to 1270 K for 1 min [heating (and cooling) rate: 5 K/s] by referring to the scanning tunneling microscope (STM) study.[2] The Auger-peak-height ratio of B(KLL)/Si(LVV) for Si(111) after heating to 1270 K was nearly saturated for the surface exposed to >0.3-L DB, and the value was 0.014 (for the primary energy of 2 keV) at the saturation in good agreement with the previous work.[16] For the Si(111) surface exposed to >0.2-L DB and heated to 1270 K, a well established $(\sqrt{3}\times\sqrt{3})R$30° LEED pattern was observed. According to these results, the $(\sqrt{3}\times\sqrt{3})R$°-B superstructure is apparently completed on Si(111) with the DB exposure of >0.3 L. In the previous studies,[2,7] however, a small amount of defects was found on the $(\sqrt{3}\times\sqrt{3})R$30°-B surface prepared by the thermal decomposition of DB on Si(111). According to the STM study,[2] the defect characteristic of the $(\sqrt{3}\times\sqrt{3})R$30°-B surface is a B deficiency at the S_5 site, where the B atom is replaced by Si. Indeed we obtained the TD and EEL spectra, which indicate that the defects exist on the $(\sqrt{3}\times\sqrt{3})R$30°-B surface formed with the DB exposure of <0.5 L. However, for the $(\sqrt{3}\times\sqrt{3})R$30°-B surface formed with the DB exposure of ≥0.5 L, no experimental evidence indicative of the defects existing on the surface was found in both TDS and EELS measurements. Thus, it is considered that the $(\sqrt{3}\times\sqrt{3})R$30°-B surface is formed with few defects by exposing Si(111) to ≥0.5-L DB and subsequent heating in our preparation procedure. In the following gas adsorption experiments, the $(\sqrt{3}\times\sqrt{3})R$30°-B surface was prepared with 0.5-L DB. Since the high-temperature heat treatment is needed in order to bring B atoms from the surface of Si(111) to the S_5 substitutional sites by breaking Si-Si bonds, it is unavoidable for a part of B atoms to diffuse deeper into the substrate. This is the reason why excess DB has to be supplied.

Figure 1(a) shows an EEL spectrum in the specular mode of the Si(111)(7×7) surface exposed to 1.5-L DB at 90 K and subsequently heated to 300 K to remove physisorbed DB (recorded at 90 K). Losses are observed at 98, 116, 189, 261, 322, and 462 meV. Essentially, little change was observed in the vibrational spectra for different exposures except for the intensity variation. The loss energies agree with the vibrational energies of solid DB (Ref. 17) (Table I), except for the 261 and 462

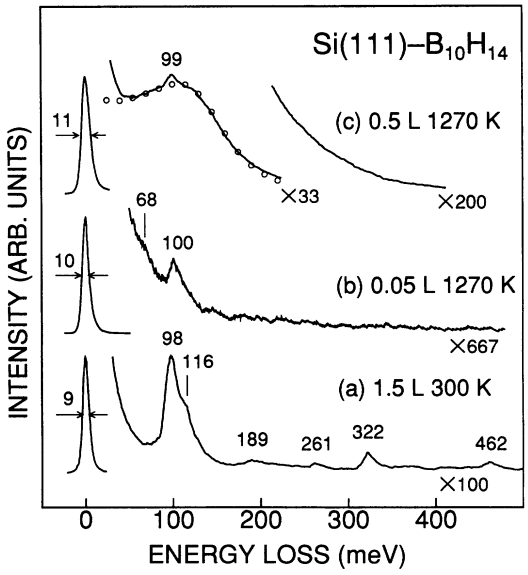

FIG. 1. (a) EEL spectrum in the specular mode of Si(111) exposed to 1.5-L $B_{10}H_{14}$ (DB) at 90 K and subsequently heated to 300 K. Primary energy $E_p=4.5$ eV. (b) and (c) EEL spectra in the specular mode of Si(111) preexposed to (b) 0.05- and (c) 0.5-L DB at 300 K and subsequently heated to 1270 K. $E_p=7.5$ eV. All the measurements were made at 90 K. Open circles represent the calculated spectrum (see text for more explanation).

TABLE I. Vibrational energies of solid $B_{10}H_{14}$ (Ref. 17) and $B_{10}H_{14}$ adsorbed on Si(111)(7×7) (meV).

Solid $B_{10}H_{14}$[a] Energy (meV)	Mode	$B_{10}H_{14}$ on Si(111)(7×7) Energy (meV)
88	B-H bending parallel to C_2 axis	
89		
93		
101		98
102	B-B skeletal stretching	
106		
113		
114		
116		116
192		189
195	B-H · · · B bridge	
197		
232		
314		
315		
318	B-H stretching	
320		322
324		
325		

[a]Only vibrational modes showing relatively strong intensities in the infrared spectrum are listed (see Ref. 17).

meV. Thus, it is concluded that DB is adsorbed nondissociatively on Si(111) at 300 K. This is consistent with the previous STM study:[2] a found disk image was observed for the DB adsorption on Si(111) at 300 K. The intensities of the 261 and 462-meV losses were observed to increase with time, and the losses are attributed to the SiH and OH stretching modes, respectively, of H_2O from the background.[18]

Figures 1(b) and 1(c) show EEL spectra in the specular mode of the Si(111) surface exposed to 0.05 and 0.5-L DB at 300 K, subsequently heated to 1270 K and cooled to 90 K, respectively. For the Si(111) surface preexposed to 0.05-L DB and heated to 1270 K, the Auger-peak-height ratio of B(*KLL*)/Si(*LVV*) was 0.005 ($\frac{1}{3}$ of saturation). For this surface, losses are observed at 68- and 100 meV [Fig. 1(b)]. Loss features associated with the SiH and BH_x species, e.g., whose energies of stretching modes are expected to be ~260 and 320 meV, respectively, are not observed. Hydrogen on the surface is desorbed by heating. The 68- and 100-meV losses are attributed to surface vibrations related to the structure having a Si adatom at the T_4 site on Si(111) along with a Si (68 meV) or B atom (100 meV) at the S_5 site. According to Northrup,[19] it is expected that two surface-phonon modes at $\bar{\Gamma}$ point are observed for the structure, which has adatoms at the T_4 sites on Si(111). One is a mode having the displacement eigenvector localized mainly on the two atoms located directly beneath the adatom, and the other a mode involving primarily the adatom and the surface Si atoms bonded to the adatom. The losses corresponding to the former were observed at 71 meV for the Si(111)(7×7) surface[20] and at 69 meV for Si(111)($\sqrt{3}\times\sqrt{3}$)R30°-Al.[21] It is interpreted that the phonon energy is shifted for the structure having B at the S_5 site due to a lighter mass of the B atom compared with Si. Thus, it is concluded that the structure having the Si adatom at the T_4 site and B at the S_5 substitutional site is formed partially on Si(111), together with that having Si atoms both at the T_4 adatom and S_5 substitutional sites. The vibrational energy of the latter mode is expected to be ~30 meV,[20–22] but we could not detect the mode.

As the surface B concentration is nearly saturated (0.5-L DB), an EEL spectrum of the surface is varied [Fig. 1(c)]. A broad and intense loss feature around ≈100 meV and a loss peak at 99 meV are observed. The 99-meV loss is the surface phonon as described above. The broad loss is not attributed to surface vibrations by referring to Fig. 1(b), but to a surface-plasmon excitation of free carriers in the near-surface region. The amount of the free carriers (and B atoms) can be estimated by analyzing the observed plasmon loss with the use of the dipole scattering theory.[13]

It is noted that the probing depth l of EELS depends on a given loss energy $\hbar\omega$:[13] $l\sim(2E_p/\hbar\omega)/k$ with $E_p=\hbar^2k^2/2m$ being a primary energy. For $E_p=7.5$ eV and $\hbar\omega\sim100$ meV, $l\sim110$ Å. We will assume that the carrier concentration n_b in the near-surface region, which is probed by electrons suffering ~100-meV energy loss, can be taken as constant. The contribution from the free carriers to the dielectric function $\epsilon(\omega)$ is given by

$$\epsilon(\omega)=\epsilon_0-\frac{4\pi n_b e^2}{m^*\omega(\omega+i/\tau)}\ , \tag{1}$$

where ϵ_0 is a bulk dielectric constant (Si:11.7), m^* an effective mass, and τ the Drude relaxation time. When the ($\sqrt{3}\times\sqrt{3}$)R30°-B superstructure is perfectly stoichiometric and ordered, surface (and defect) states do not exist in the bulk band gap. In this case, the Fermi-level pinning does not occur, and the flat-band condition exists near the surface.[23] The contribution from the surface optical phonon will be ignored here.

Under the above conditions, the electron-energy-loss probability $P(\mathbf{k},\mathbf{k}')d\Omega_{\mathbf{k}'}d(\hbar\omega)$, that an incident electron is scattered into the range of energy losses between $\hbar\omega$ and $\hbar(\omega+d\omega)$ and into the solid angle $d\Omega_{\mathbf{k}'}$ around the direction of $\mathbf{k}'$, is given by[13]

$$P(\mathbf{k},\mathbf{k}')=A(\mathbf{k},\mathbf{k}')(n_\omega+1)\mathrm{Im}\left[\frac{-1}{1+\epsilon(\omega)}\right]\ , \tag{2}$$

where $\mathbf{k}$ and $\mathbf{k}'$ are the wave vectors of an incident and scattered electron; $\hbar^2(k^2-k'^2)/2m=\hbar\omega$, n_ω the Bose-Einstein factor, and $A(\mathbf{k},\mathbf{k}')$ a kinematic factor defined by $\mathbf{k}$ and $\mathbf{k}'$.[14] Actually, the measured loss intensity is proportional to $P(\mathbf{k},\mathbf{k}')$ integrated over the solid angle subtended by the entrance slit of the analyzer. The analyzer of our EEL spectrometer consists of a 127° cylindrical deflector with an entrance slit shaped rectangularly. In the following calculation, the kinematic factor A was integrated over $|\alpha|\le0.5°$ and $|\beta|\le3°$, where the in-plane angle α is the difference between the incidence

angle θ_i and the angle θ_s, which is the angle between the projection of $\mathbf{k}'$ onto the scattering plane and the surface normal, and the out-of-plane angle β the angle between $\mathbf{k}'$ and its projection onto the scattering plane.[24] These angles were determined consistently with the experiments.

The fitting parameters are the carrier concentration n_b of the *substrate* and the Drude relaxation time τ assuming the hole effective mass m^* of $0.35m$.[25] Open circles in Fig. 1(c) show an EEL spectrum calculated by using Eq. (2) with n_b of 7.0×10^{19} cm^{-3} and τ of 5.5×10^{-15} s. The calculated spectrum agrees well with the observed one in spite of the assumptions made in the calculation. In the course of fitting, we have found that similar results are obtained for the in-plane angular apertures ranging from $|\alpha|\leq0.4°$ to $|\alpha|\leq3°$, and that both n_b and τ are decreased at most 10% with expanding the aperture size.

The evaluated value of n_b is much larger than the intrinsic carrier concentration of 5×10^{18} cm^{-3} at 1270 K. Thus, the diffusion of B atoms into the substrate is the extrinsic one.[26] The diffusion length is 1.2×10^3 Å assuming the *constant* surface concentration of 7×10^{19} cm^{-3}, the heating temperature of 1270 K, and the heating time of 60 s.[26] The length is the lowest limit of the actual one. Therefore, the first assumption made in the calculation of the plasmon profile, that n_b is constant in the near-surface region, gives a good approximation. Further, the large value of n_b implies that freeze-out of carriers does not occur and that the concentration can be regarded as that of diffused B atoms. It is noted that n_b evaluated for our sample is 3.5 times as large as that for the $(\sqrt{3}\times\sqrt{3})R30°$-B surface prepared by Chen, Colaianni, and Yates.[16] It is considered that the larger concentration suppresses the production of the B deficiency in the $(\sqrt{3}\times\sqrt{3})R30°$-B layer. Thus, our sample is expected to have fewer defects than that prepared by them. With τ of 5.5×10^{-15} s and m^* of $0.35m$, the mobility in the near-surface region is estimated to be 28 cm^{2}V^{-1}s^{-1}. This is $\sim\frac{1}{2}$ of the bulk value corresponding to the same impurity concentration ($\sim$50 cm^{2}V^{-1}s^{-1} at 300 K).[26] It is considered that this is related to the short heating time in the preparation and that a large number of imperfections may exist in the near-surface region.

We have found that the quasielastic-peak width of the EEL spectra of the $Si(111)(\sqrt{3}\times\sqrt{3})R30°$-B surface depends on the sample temperature. The full width at half maximum (FWHM) of the quasielastic peak of the EEL spectra of the $(\sqrt{3}\times\sqrt{3})R30°$-B surface formed with 0.5-L DB is shown as a function of temperature by open circles in Fig. 2. The quasielastic-peak width is increased almost linearly with temperature in the measured range from 90 to 370 K. It is possible to obtain the total number of free carriers in the near-surface region by analyzing the quasielastic peak. Losses involved in the quasielastic peak are a few meV, and thus $l>10^3$ Å. The length is so large that all free carriers introduced by the short-time heating adopted in our preparation procedure may be included.

For the quasielastic-peak profile, Persson and coworkers[14,15] have derived a simple formula, taking account of multiple scattering, which becomes important

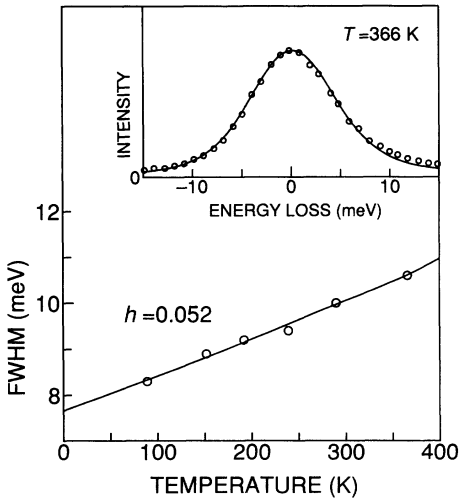

FIG. 2. Temperature dependence of the width (FWHM) of the quasielastic peak for the $Si(111)(\sqrt{3}\times\sqrt{3})R30°$-B surface. The experimental reseults are shown by open circles and the calculated results (for $h=0.052$) by the solid curve. $E_p=7.5$ eV. The inset shows the experimental (open circles) and calculated (solid curve) profiles of the quasielastic peak at 366 K.

for very small loss energies, i.e., below a few tens meV. According to Persson and co-workers,[14,15] the quasielastic-peak profile $P(\omega)$ is given by

$$P(\omega)\simeq\frac{1}{\pi}\left[\frac{\Gamma/2}{\omega^2+(\Gamma/2)^2}\cos\phi+\frac{\omega}{\omega^2+(\Gamma/2)^2}\sin\phi\right], \quad (3)$$

where $\Gamma=4Chk_BT$, $\phi=Ch$,

$$C=\frac{4}{\pi}\frac{1}{\cos^2\theta_i}\frac{1}{ka_0}\frac{1}{\epsilon_0+1}, \quad (4)$$

$$h(1/\beta\tau,\theta_i)=\int_0^\infty dx\, f(x,\theta_i)\frac{1/\beta\tau}{(1/\beta\tau)^2+x^2(1-1/\epsilon_0)^2}, \quad (5)$$

$$\beta=\frac{4\pi ne^2}{m^*(\epsilon_0+1)}\frac{1}{v}, \quad (6)$$

and

$$f(x,\theta_i)=\frac{1}{x}\int_0^{2\pi}d\phi\left[1+\left[\frac{1/x}{\cos\theta_i}-\tan\theta_i\cos\phi\right]^2\right]^{-2}. \quad (7)$$

In these expressions, θ_i is an electron incidence angle with respect to the surface normal, k_B the Boltzmann constant, a_0 the Bohr radius, n a carrier concentration *per unit area,* and v a velocity of an incident electron. Equation (3) holds if (i) almost all inelastically scattered electrons pass into the analyzer, which is met for very small loss energies in the specular-mode measurements, (ii) $\hbar\beta\gg\hbar\omega$, and (iii) $Ch/\pi\ll1$. $C=0.76$ for $E_p=7.5$ eV and $\theta_i=65°$. The last two conditions are satisfied in

the present case, which will be found shortly. It is noted that the broadening of the quasielastic peak for the $(\sqrt{3}\times\sqrt{3})R30°$-B surface is a direct consequence of the Drude damping from the condition (ii), contrary to that for the Si(111)(7×7) surface caused by multiple excitation of low-energy two-dimensional plasma oscillation.[14]

The temperature dependence of the quasielastic-peak width is calculated using Eq. (3) and compared with the experiment (Fig. 2). It is obvious from Eq. (3) that there is only a single fitting parameter h, which is a function of $1/\beta\tau$. The solid line in Fig. 2 shows the calculation carried out for $h=0.052$ ($1/\beta\tau=0.033$) independent of temperature. The spectrometer window is assumed to be a Gaussian of 7.7-meV FWHM. The agreement between the calculation and experiment is good. The reason why h is independent of the temperature is that the population of free carriers is concentrated in the high B-concentration region near the surface and that both carrier concentration and mobility are almost independent of temperature for very high B concentration, say $\geq 10^{19}$ cm^{-3}.[27] The inset of Fig. 2 shows the experimental (open circles) and calculated (solid curve) profile of the quasielastic peaks at 366 K. By using $1/\beta\tau$ of 0.033 and τ of 5.5×10^{-15} s, $\hbar\beta=3.6$ eV, and the total number of free carriers introduced near surface region is estimated to be 1.2×10^{15} cm^{-2}.

B. Si(111)$(\sqrt{3}\times\sqrt{3})R30°$-B/$NH_3$

TDS measurements after exposing the Si(111)$(\sqrt{3}\times\sqrt{3})R30°$-B surface to NH_3 at 95 K showed that NH_3 was the only desorption product and H_2 was not detected. This suggests that NH_3 is adsorbed nondissociatively and is not decomposed thermally on the surface. TD spectra for the $(\sqrt{3}\times\sqrt{3})R30°$-B surface exposed to an increasing amount of NH_3 at 95 K are shown in Fig. 3 (heating rate was 2.5 K/s). For small exposures (<1 L), three desorption peaks are observed at ~115, 140, and 170 K. No peak was observed at higher temperatures. The ~115-K peak intensity is increased with increasing exposure. The other peaks are merged into the tail of this peak, which results from the slow pumping of NH_3 in the neighborhood of the ionization chamber of the mass spectrometer. The rising edges of the ~115-K peak are common in the TD spectra of Fig. 3, and the peak is shifted to higher temperature with increasing exposure. These indicate the zeroth-order desorption, and the ~115-K peak is attributed to the desorption from a bulklike multilayer. Similar desorption spectra, showing three intact desorption peaks, were observed for NH_3 adsorbed on metals. For example, Gland, Sexton, and Mitchell[28] observed the NH_3 desorption peaks at 109, 122, and 180 K for the Ag(110)-NH_3 system, which were assigned to the NH_3 multilayer, NH_3 hydrogen bonded to a chemisorbed NH_3, and molecularly chemisorbed NH_3, respectively. EELS measurements indicate that chemisorbed NH_3 exists on the $(\sqrt{3}\times\sqrt{3})R30°$-B surface at low temperatures, as will be described later. The heats of desorption for the 140 and 170-K peaks are estimated to be 8 and 10 kcal/mol, respectively, by the use of the Redhead formula[29] assuming a first-order desorption and a preexponential factor of 10^{13} s^{-1}. Thus, the 140 and 170-K peaks seen in Fig. 3 are attributed to NH_3 hydrogen bonded to a chemisorbed NH_3 and molecularly chemisorbed NH_3 on the $(\sqrt{3}\times\sqrt{3})R30°$-B surface, respectively.

Figures 4(a) and 4(b) show EEL spectra measured in the specular and off-specular ($\Delta\theta=3°$; see the inset of Fig. 4 for the definition of the off-specular angle $\Delta\theta$) modes for the Si(111)$(\sqrt{3}\times\sqrt{3})R30°$-B surface exposed to 5-L NH_3 at 90 K, respectively. For smaller exposures ($\lesssim1$

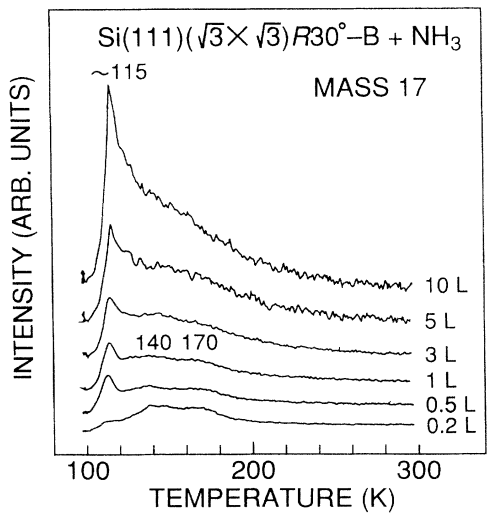

FIG. 3. TD spectra of NH_3 (mass 17) from the Si(111)$(\sqrt{3}\times\sqrt{3})R30°$-B surface exposed to various amounts of NH_3 at 95 K. The heating rate was 2.5 K/s.

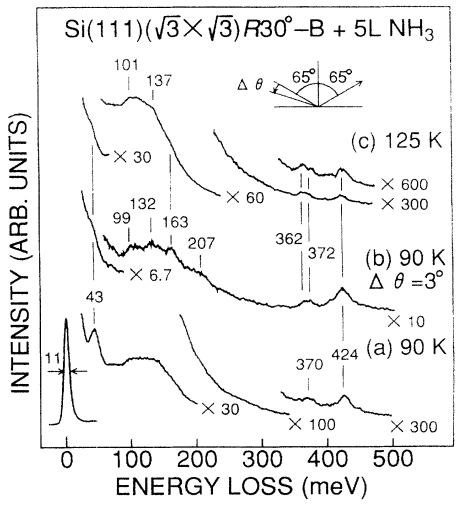

FIG. 4. EEL spectra of the Si(111)$(\sqrt{3}\times\sqrt{3})R30°$-B surface exposed to 5-L NH_3 at 90 K [(a) $\Delta\theta=0°$, (b) $\Delta\theta=3°$], and (c) subsequently heated to 125 K (heating rate was 2.5 K/s) and cooled to 90 K ($\Delta\theta=0°$). $E_p=7.5$ eV. The off-specular angle $\Delta\theta$ is shown in the inset.

L), the losses associated with the $(\sqrt{3}\times\sqrt{3})R30°$-B surface were found to predominate and those associated with adsorbed NH_3 were difficult to be resolved. Losses associated with adsorbed NH_3 on the $(\sqrt{3}\times\sqrt{3})R30°$-B surface are resolved at 43, ~370, and 424 meV in the specular-mode spectrum [Fig. 4(a)], and at 43, 132, 163, 207, 362, 372, and 424 meV in the off-specular-mode spectrum [Fig. 4(b)]. By comparing Figs. 4(a) with 4(b), it is considered that the 43-meV loss is excited mainly by the dipole scattering mechanism and that the ~370 and 424-meV losses mainly by the impact mechanism.[13] As NH_3 is adsorbed on the $(\sqrt{3}\times\sqrt{3})R30°$-B surface, the intensity of the plasmon loss relative to that of the elastic peak is decreased, and the spectral profile around 85–150 meV is changed [Figs. 1(c) and 4(a)]. One reason for the decreased intensity of the plasmon loss is the screening by the overlayer of NH_3 adsorbed on the surface. Since the surface-phonon loss, which is clearly resolved in Fig. 1(c), is merged into the loss feature around 85–150 meV in Fig. 4(a) and losses associated with adsorbed NH_3 are observed in this loss energy region, the loss feature around 85–150 meV has some contribution from losses of adsorbed NH_3. The spectral profile of the plasmon loss may be varied by some change in the surface electronic states induced by the NH_3 adsorption. This has prevented us from deciding how to subtract the background of the plasmon loss for the other losses and by what mechanism the other losses are excited. Thus, we will not make any discussion about the observed losses by the excitation mechanisms.

The 43-, 132-, 207-, and 424-meV losses are close to vibrational energies of gas- or solid-phase NH_3 (Refs. 30 and 31) (Table II), and are attributed to the hindered rotation, symmetric deformation, degenerate deformation, and (symmetric and) degenerate stretching modes of physisorbed NH_3, respectively. It is considered that these losses also have contributions from the vibrational modes of NH_3 hydrogen bonded to the chemisorbed molecule, as will be described later.

The energies of the 163- and ~370-meV losses are markedly different from any vibrational energies of free NH_3, and the losses are attributed to the vibrational modes of chemisorbed NH_3 on the $(\sqrt{3}\times\sqrt{3})R30°$-B surface. Since the SiH stretching mode is not observed, NH_3 is chemisorbed nondissociatively on the surface. This is consistent with the TDS results. The 163-, 362-, and 372-meV losses are attributed to the symmetric deformation, symmetric stretching, and degenerate stretching modes, respectively. According to the infrared and Raman spectroscopy studies of metal ammine complexes,[32] NH_3 in the complexes has the vibrational energies of the symmetric deformation, symmetric stretching, and degenerate stretching modes at 135–170, 378–404, and 391–416 meV, respectively (Table II). For example, $[Pt(NH_3)_6]Cl_4$ has the corresponding energies at 170, 378, and 391 meV, respectively.[32] Thus, it is concluded that chemisorbed NH_3 is coordinated to the $(\sqrt{3}\times\sqrt{3})R30°$-B surface. Because the Si adatom is charged positively owing to the charge transfer to the B atom,[2–4] it is considered that the chemisorbed state similar to the coordinate bonding to metal ions is realized on the $(\sqrt{3}\times\sqrt{3})R30°$-B surface. The same conclusion has been reached by Avouris *et al.*[2]

One might attribute the NH_3 stretching modes of ~370 meV, which are significantly lowered from the values of free NH_3, to the hydrogen-bonding interaction with adsorbed NH_3 molecules or that with the surface Si atom(s).[13] The former case can be readily excluded by comparing the energies of gas- and solid-phase NH_3 listed in Table II. With respect to the latter case, the ~370-meV-loss band has a peak width similar to that of the 424-meV loss, and the ~370- and 424-meV losses are clearly resolved. Further, the corresponding significant lowering of the CH stretching modes were not observed for the $Si(111)(\sqrt{3}\times\sqrt{3})R30°$-B/$C_6H_6$ system (Sec. III C). Thus, the possibility can be excluded.

The losses related to the other vibrational modes of chemisorbed NH_3 are not resolved, possibly due to the vibrational energies, which are close to those of physisorbed NH_3 or surface phonon, and/or due to the small dynamic dipole moments of the modes.

Figure 4(c) shows an EEL spectrum in the specular mode of the $(\sqrt{3}\times\sqrt{3})R30°$-B surface exposed to 5-L NH_3 at 90 K, and subsequently heated to 125 K (and cooled to 90 K). Changes in relative intensities among losses, especially between the ~370- and 424-meV-loss

TABLE II. Vibrational energies of NH_3 (meV). l = hindered rotation, ρ_r = rocking, δ = deformation, ν = stretching, s = symmetric, d = degenerate, and X = substrate.

Mode	NH_3 gas (Ref. 30)	NH_3 solid (Ref. 31)	Metal-NH_3 complexes (Ref. 32)	On $Si(111)(\sqrt{3}\times\sqrt{3})R30°$-B Physisorbed NH_3	Chemisorbed NH_3
$l(NH_3)$		45		43	
$\rho_r(NH_3)$			73–118		
$\delta_s(NH_3)$	118	131	135–170	132	163
$\delta_d(NH_3)$	202	204	194–207	207	
$\nu_s(NH_3)$	414	400	378–404		362
$\nu_d(NH_3)$	423	419	391–416	424	372
$\nu(X\text{-}NH_3)$			30–71		

bands, are observed [Figs. 4(a) and 4(c)]. By referring to the TDS results (Fig. 3), the NH_3 multilayer is removed by the heating to 125 K, and there exist on the surface NH_3 hydrogen bonded to chemisorbed one and chemisorbed NH_3 molecule on the surface, corresponding to the 140- and 170-K desorption peaks, respectively. The 424-meV loss is decreased in intensity but still observed by heating to 125 K. This indicates that the loss is related to the (symmetric and) degenerate stretching mode not only of NH_3 in the multilayer but also of NH_3 hydrogen bonded to the chemisorbed molecule. Similarly, the 43-, 132-, 163-, and 207-meV losses are considered to have contribution from the vibrational modes of NH_3 hydrogen bonded to chemisorbed one. Further, the 424-meV loss has the intensity almost equal to that of the ~370-meV loss. This may be related to the TDS result that the desorption peaks at 140 and 170 K have similar area intensities (Fig. 3). Vibrational losses associated with adsorbed NH_3 were difficult to observe after heating to higher temperatures, because the population of adsorbed NH_3 was decreased and the losses related to the $(\sqrt{3}\times\sqrt{3})R30°$-B surface again predominated. The clean-surface spectrum was obtained after heating to >200 K.

Figures 5(a) and 5(b) show EEL spectra in the specular mode with a higher primary energy of 12 eV of the $(\sqrt{3}\times\sqrt{3})R30°$-B surface before and after 5-L NH_3 exposure at 90 K, respectively. Losses are observed at 2.0 eV for the $(\sqrt{3}\times\sqrt{3})R30°$-B surface [Fig. 5(a)], and at 0.43 and 0.86 eV for the $(\sqrt{3}\times\sqrt{3})R30°$-B surface exposed to NH_3 [Fig. 5(b)]. By comparison with Fig. 4, the 0.43- and 0.86-eV losses are attributed to the stretching mode of NH_3 in the multilayer and NH_3 hydrogen bonded to chemisorbed one and the overtone (and multiple loss), respectively. The losses associated with the ~370-meV loss observed in Fig. 4 are not observed due to the weaker intensity compared with the 424-meV-loss intensity and also to the degraded resolution of the spectrometer (80-meV FWHM). Referring to the surface band dispersion of the $(\sqrt{3}\times\sqrt{3})R30°$-B surface,[4] the 2.0-eV loss is attributed to a one-electron transition from an occupied backbond state to an empty dangling-bond state. Similar electronic transition was observed for the Si(111)$(\sqrt{3}\times\sqrt{3})R30°$-Al surface.[33] It is noted that the 2.0-eV loss disappears upon NH_3 adsorption. This indicates that the initially empty dangling-bond orbital is involved in the NH_3 chemisorption. The corresponding loss is still observed for ~3 ML of C_6H_6 physisorbed on the $(\sqrt{3}\times\sqrt{3})R30°$-B surface (assuming that the saturation of the α_1 layer, which will be described later, corresponds to 1 ML) [Fig. 5(c)]. It is interpreted that the interaction of the dangling-bond orbital of the Si adatom with the lone-pair $3a_1$ orbital of NH_3 lifts up an unoccupied antibonding orbital having mainly the dangling-bond character, and the 2.0-eV loss disappears. The large Coulomb repulsion is expected when an electron is excited into the antibonding orbital having large overlap in space with the bonding orbital, which already accommodates two electrons. The loss corresponding to the electronic transition observed for the $(\sqrt{3}\times\sqrt{3})R30°$-B surface at 2.0 eV may be merged into the substrate transitions or lifted to the energy higher than the loss-energy region measured.

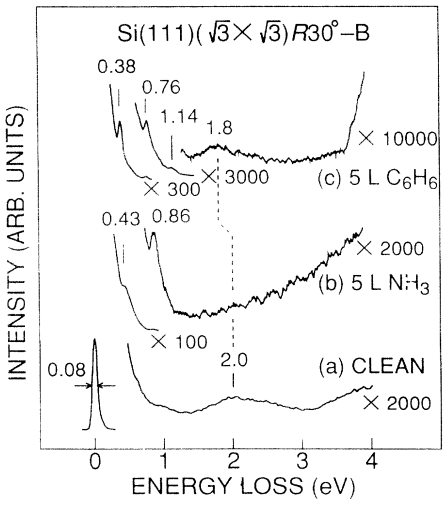

FIG. 5. EEL spectra in the specular mode of (a) the clean Si(111)$(\sqrt{3}\times\sqrt{3})R30°$-B surface at 90 K; (b) and (c), the Si(111)$(\sqrt{3}\times\sqrt{3})R30°$-B surface exposed to 5-L NH_3 and 5-L C_6H_6 at 90 K, respectively. $E_p = 12$ eV.

Since NH_3 is chemisorbed by donating lone-pair electrons to the Si adatom, it is considered that charge transferred to the B atom does not turn back to the Si adatom, different from the interaction of the Si(111)(7×7) surface with NH_3.[34]

The chemisorbed state of NH_3 on the $(\sqrt{3}\times\sqrt{3})R30°$-B surface is quite different from those on the Si(111)(7×7) (Ref. 8) and Si(100)(2×1) (Ref. 9) surfaces, where NH_3 is dissociated to form $SiNH_2$ and SiH species. The markedly decreased vibrational energies of the stretching modes of NH_3 chemisorbed on the $(\sqrt{3}\times\sqrt{3})R30°$-B surface indicates that the N-H bonds are significantly weakened. If there were another active site appropriate for extracting H atom of NH_3 near the NH_3-chemisorbed Si adatom, NH_3 would be dissociated with the molecularly chemisorbed state as a precursor state of the reaction. However, there is only a single kind of the Si adatom on the $(\sqrt{3}\times\sqrt{3})R30°$-B surface, which is electrophile as mentioned above. Further, the distance between the neighboring Si adatoms is 6.7 Å, which is larger than those between active sites on clean Si surfaces. These are the reasons why NH_3 is not dissociated on the $(\sqrt{3}\times\sqrt{3})R30°$-B surface.

C. Si(111)$(\sqrt{3}\times\sqrt{3})R30°$-B/$C_6H_6$

TDS measurements after exposing the Si(111)$(\sqrt{3}\times\sqrt{3})R30°$-B surface to C_6H_6 at 95 K showed that C_6H_6 was the only desorption product. Figure 6 shows TD spectra for the $(\sqrt{3}\times\sqrt{3})R30°$-B surface exposed to an increasing amount of C_6H_6 at 95 K (heating rate was 2.5 K/s). Three desorption peaks are observed

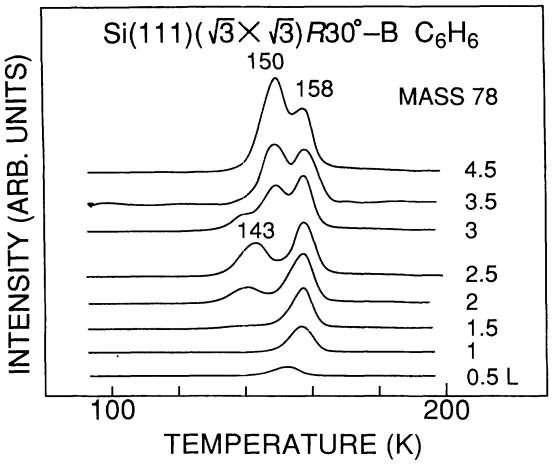

FIG. 6. TD spectra of C_6H_6 (mass 78) from the Si(111)$(\sqrt{3}\times\sqrt{3})R30°$-B surface exposed to various amounts of C_6H_6 at 95 K. The heating rate was 2.5 K/s.

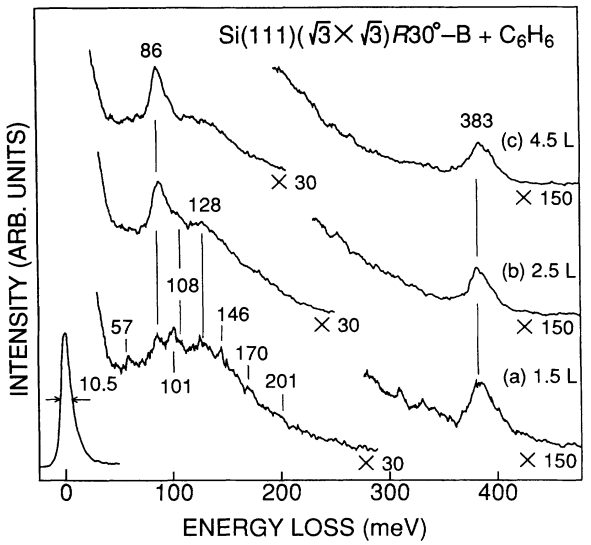

FIG. 7. EEL spectra in the specular mode of the Si(111)$(\sqrt{3}\times\sqrt{3})R30°$-B surface exposed to various amounts of C_6H_6 at 90 K: (a) 1.5 L, (b) 2.5 L, and (c) 4.5 L exposures. $E_p = 7.5$ eV.

at 143, 150, and 158 K. No desorption peaks were observed at >200 K. The characteristic behavior of these peaks with increasing exposure is similar to that for benzene physisorbed on Si(111)(7×7) (Ref. 10) and on some transition metals, e.g., on Ru(001).[35] Thus, these peaks are attributed to desorption of C_6H_6 physisorbed on the surface. The fact that only desorption of physisorbed C_6H_6 is observed suggests that C_6H_6 does not chemisorb on the $(\sqrt{3}\times\sqrt{3})R30°$-B surface. The same conclusion has been obtained from EELS measurements as will be described later.

Following the labels used by Polta and Thiel,[36] the three peaks seen in Fig. 6 are associated with the α_1 (highest-temperature peak), α_2 (lowest temperature), and α_3 (intermediate temperature) layers. It is interesting to see that the desorption peak associated with the α_1 layer is observed for physisorbed C_6H_6 on the $(\sqrt{3}\times\sqrt{3})R30°$-B surface, though the chemisorbed layer does not exist on the surface. The α_1 layer formed on Si(111)(7×7) (Ref. 10) or transition metal[35] is the first physisorbed layer on top of the chemisorbed layer. Benzene in the α_1 layer on those surfaces interacts electrostatically with the chemisorbed molecule polarized by being π bonded to those surfaces, and desorbs at the temperature higher than those from the other two layers. It is interpreted that the first physisorbed C_6H_6 on the $(\sqrt{3}\times\sqrt{3})R30°$-B surface interacts electrostatically with the positively charged Si adatom in place of the polarized chemisorbed molecule.

Figure 7 shows EEL spectra in the specular mode of the $(\sqrt{3}\times\sqrt{3})R30°$-B surface exposed to 1.5, 2.5, and 4.5-L C_6H_6 at 90 K, respectively. Losses associated with adsorbed C_6H_6 on the $(\sqrt{3}\times\sqrt{3})R30°$-B surface are observed. The loss energies are close to those of gas-, liquid-, or solid-phase C_6H_6,[30] and are attributed to vibrational modes of physisorbed C_6H_6 on the $(\sqrt{3}\times\sqrt{3})R30°$-B surface. The assignments are summarized in Table III. The numbering system of Herzberg[37] is used in the table. A loss associated with the SiH stretching mode and losses that can be ascribed to the vibrational modes of chemisorbed C_6H_6 were not observed. By referring to the TDS results (Fig. 6), EEL spectra of Figs. 7(a), 7(b), and 7(c) are related to the α_1, $\alpha_1+\alpha_2$, and $\alpha_1+\alpha_3$ layers, respectively.

As the C_6H_6 exposure is increased, the 86-meV-loss in-

TABLE III. Vibrational energies (meV) and their assignments of C_6H_6 physisorbed on the Si(111)$(\sqrt{3}\times\sqrt{3})R30°$-B surface at 90 K together with those of gas-, liquid-, or solid-phase C_6H_6 (Ref. 30). The mode number and representation (D_{6h} symmetry) are included.

			Vibrational energies (meV)	
Mode number	Repr.	Mode	Gas-, liquid-, or solid-phase C_6H_6	C_6H_6 on Si(111) $(\sqrt{3}\times\sqrt{3})R30°$-B
ν_{20}	(E_{2u})	γ_{CC}	51	57
ν_4	(A_{2u})	γ_{CH}	83	86
ν_{11}	(E_{1g})	γ_{CH}	105	108
ν_2	(A_{1g})	δ_{CC}	123	
ν_7	(B_{2g})	γ_{CH}	123	
ν_{14}	(E_{1u})	δ_{CH}	129	128
ν_{10}	(B_{2u})	δ_{CH}	143	
ν_{17}	(E_{2g})	δ_{CH}	146	146
ν_3	(A_{2g})	δ_{CH}	164	170
ν_{16}	(E_{2g})	ν_{CC}	198	201
ν_{15}	(E_{2g})	ν_{CH}	378	
ν_1	(A_{1g})	ν_{CH}	380	
ν_{12}	(E_{1u})	ν_{CH}	380	383
ν_5	(B_{1u})	ν_{CH}	380	

γ=out-of-plane bending, δ=in-plane bending, and ν=stretching.

tensity is clearly increased in comparison with the intensities of the other losses of physisorbed C_6H_6. The off-specular measurements indicate that the 86-meV loss is predominantly excited by the dipole scattering. As shown in Table III, the loss is attributed to the out-of-plane CH bending mode, which has the dynamic dipole moment perpendicular to the carbon ring. Thus, it is considered that the mean angle with respect to the surface of the molecular plane of C_6H_6 physisorbed on the $(\sqrt{3}\times\sqrt{3})R\,30°$-B surface is largest in the α_1 layer and decreases with increasing exposure. The fact that the mean tilt angle for the α_2 layer is smaller than that for the α_1 layer is consistent with the TDS results: Contrary to the TD spectra observed for physisorbed benzene on Si(111)(7×7) (Ref. 10) or transition metal,[35] the maximum area intensity of the α_2 desorption peak observed in Fig. 6 is smaller than that of the α_1 peak. Benzene physisorbed on Ru(001) (Ref. 35) [and possibly on Si(111)(7×7)] is oriented parallel to the surface in the α_1 layer, and tilted with a high mean angle in the α_2 layer. The orientation of C_6H_6 physisorbed on the $(\sqrt{3}\times\sqrt{3})R\,30°$-B surface shows an opposite trend. It is considered that the high mean tilt angle for C_6H_6 in the α_1 layer is associated with the size of Si adatom, which is smaller than that of chemisorbed benzene. C_6H_6 may be tilted (possibly standing nearly vertically) in order to interact electrostatically with the Si adatom in the most effective way.

Figure 5(c) shows an EEL spectrum in the specular mode of the $(\sqrt{3}\times\sqrt{3})R\,30°$-B surface exposed to 5-L C_6H_6 at 90 K. By referring to the TDS results, this exposure corresponds to the formation of ~3 ML of physisorbed C_6H_6. Losses are observed at 0.38, 0.76, 1.14, and 1.8 eV. The narrow losses at 0.38, 0.76, and 1.14 eV are attributed to the CH stretching mode and its overtones (and multiple losses) by comparing to Fig. 7. The loss feature rising sharply from ~4 eV is attributed to an onset of the intramolecule $\pi\rightarrow\pi^*$ electronic transition of C_6H_6.[38] The 2.0-eV loss observed for the $(\sqrt{3}\times\sqrt{3})R\,30°$-B surface is lowered by 0.2 eV and is decreased in intensity upon C_6H_6 adsorption. Possibly, the loss-energy shift of the electronic transition from the backbond to dangling-bond state may be owing to the electrostatic interaction of Si adatom with C_6H_6 in the α_1 layer, and the decrease in intensity may be due to the adsorbed layer formed on $(\sqrt{3}\times\sqrt{3})R\,30°$-B.

Benzene chemisorbs on the Si(111)(7×7) (Ref. 10) and Si(100)(2×1) (Ref. 11) surfaces, but does not on the Si(111)$(\sqrt{3}\times\sqrt{3})R\,30°$-B surface. This is considered to be associated with the delocalization of π electrons involved in the reactions. As described in Sec. III B, the $(\sqrt{3}\times\sqrt{3})R\,30°$-B surface is not suitable for the dissociative reaction of a gas molecule, and only the nondissociative adsorption is expected. If benzene were to bond to the Si adatom on the surface, the molecule would lose a part of the resonance energy (36 kcal/mol[39]). It is considered that the loss in the resonance energy is compensated by the saturation of the dangling bond(s) on Si(111)(7×7) and Si(100)(2×1) surfaces and benzene does chemisorb on these surfaces. On the other hand, the dangling-bond level of the Si adatom on the $(\sqrt{3}\times\sqrt{3})R\,30°$-B surface is initially empty. The bond formation between benzene with the adatom would compensate a loss in the resonance energy only insufficiently, and thus, benzene does not chemisorb on the $(\sqrt{3}\times\sqrt{3})R\,30°$-B surface.

It is worth noting that the reactivity criterion of the $(\sqrt{3}\times\sqrt{3})R\,30°$-B surface may be given by considering both absolute electronegativity and nature of orbitals of a molecule, which interacts with the surface.[12] Since the dangling-bond level of the Si adatom on the surface is empty, an electron donation from a molecule (or atom) to the adatom, i.e., an action as a Lewis base, should be required for the chemisorption on the $(\sqrt{3}\times\sqrt{3})R\,30°$-B surface. It is possible to tell whether a molecule donates electron(s) to the adatom or not, by examining a quantity χ called the absolute electronegativity. The definition of χ is

$$\chi=(I+A)/2=-\mu\ , \tag{8}$$

where I is the ionization potential, A the electron affinity, and μ the chemical potential.[12] If a molecule has a value of χ smaller than that of the Si adatom, the molecule will donate the electron(s). Though the van der Waals interaction with the $(\sqrt{3}\times\sqrt{3})R\,30°$-B surface may modify the value of χ of a molecule from that of the free one, the value of a free molecule gives a crude estimation. We assume tentatively $\chi=4.6$ for the Si adatom, which is equal to the work function of the $(\sqrt{3}\times\sqrt{3})R\,30°$-B surface.[40] Including the results obtained in this work, it has been found up to now that ammonia and potassium atom[23,41] chemisorb on the $(\sqrt{3}\times\sqrt{3})R\,30°$-B surface while atomic hydrogen,[5] oxygen,[6] and benzene do not. The values of χ are 2.6, 2.4, 7.2, 6.3, and 4.1 for NH_3, K, H, O_2, and C_6H_6, respectively.[12] The prediction based on the values of χ for the chemisorption on the $(\sqrt{3}\times\sqrt{3})R\,30°$-B surface is correct, except for C_6H_6. Benzene is a π base while the Si adatom has the accepting orbital of σ type. Thus, the reaction between them is considered to be unfavorable. According to the above discussion, for example, it is expected that H_2O ($\chi=3.1$)[12] chemisorbs on the $(\sqrt{3}\times\sqrt{3})R\,30°$-B surface, while CO ($\pi$ acid and $\chi=6.1$)[12] does not. For reactions on clean Si surfaces, it is unfortunately impossible to apply this simple criterion. Since the dangling-bond levels of the clean surfaces are partially filled, electron(s) may flow both from a molecule to the surface Si atom and in the opposite direction upon chemisorption.

IV. SUMMARY

We have studied the adsorbed states of NH_3 and C_6H_6 on the Si(111)$(\sqrt{3}\times\sqrt{3})R\,30°$-B surface by using thermal-desorption spectroscopy and both vibrational and electronic electron-energy-loss spectroscopy.

(1) There exist NH_3 in the multilayer, NH_3 hydrogen bonded to a chemisorbed NH_3, and chemisorbed NH_3 on the $(\sqrt{3}\times\sqrt{3})R\,30°$-B surface at 90 K. These desorb at ~115, 140, and 170 K, respectively. The N-H bonds of chemisorbed NH_3 are significantly weakened compared with those of free NH_3. Upon NH_3 adsorption, the 2.0-

eV electronic transition from the backbond state to the dangling-bond state of the Si adatom on the $(\sqrt{3}\times\sqrt{3})R30°$-B surface is removed. It is proposed that chemisorbed NH_3 is coordinated to the Si adatom on the surface by the interaction of the lone-pair orbital with originally empty dangling-bond orbital of the Si adatom. The chemisorbed state of NH_3 on the $(\sqrt{3}\times\sqrt{3})R30°$-B surface is significantly different from those on clean Si surfaces, which have been studied, and the reason is discussed.

(2) C_6H_6 physisorbs on the $(\sqrt{3}\times\sqrt{3})R30°$-B surface at <160 K. The physisorbed layer consists of three different layers. C_6H_6 in the α_1 layer first physisorbed on the surface has the highest mean tilt angle and interacts with the Si adatom electrostatically. Contrary to the interactions with clean Si surfaces, C_6H_6 does not chemisorb on the $(\sqrt{3}\times\sqrt{3})R30°$-B surface, and the reason is discussed. We have shown that the concept of the absolute electronegativity can be applied to the interactions of the $(\sqrt{3}\times\sqrt{3})R30°$-B surface with molecules or atoms.

(3) We have also analyzed the electron-energy-loss spectra of the $(\sqrt{3}\times\sqrt{3})R30°$-B surface by the use of the dipole scattering theory, and the information on the free carriers, which was introduced by the high-temperature heating in the preparation of the surface, was obtained. For the $(\sqrt{3}\times\sqrt{3})R30°$-B surface having few defects, the carrier density of 7×10^{19} cm^{-3} and Drude relaxation time of 5.5×10^{-15} s in the vicinity of the surface were evaluated by the analysis of the plasmon loss, and the total number of 1×10^{15} cm^{-2} was estimated by that of the quasielastic peak.

ACKNOWLEDGMENTS

One of the authors (Y.T.) thanks Professor O. Aita for encouragement in writing this manuscript. This work was supported in part by the Grant-in-Aid for Scientific Research from the Ministry of Education.

*Author to whom all correspondence should be addressed. FAX: +81-722-59-3340.

[1]V. V. Korobtsov, V. G. Lifshits, and A. V. Zotov, Surf. Sci. **195**, 466 (1988).
[2]Ph. Avouris, I.-W. Lyo, F. Bozso, and E. Kaxiras, J. Vac. Sci. Technol. A **8**, 3405 (1990).
[3]E. Kaxiras, K. C. Pandey, F. J. Himpsel, and R. M. Tromp, Phys. Rev. B **41**, 1262 (1990).
[4]T. M. Grehk, P. Mårtensson, and J. M. Nicholls, Phys. Rev. B **46**, 2357 (1992).
[5]P. J. Chen, M. L. Colaianni, and J. T. Yates, Jr., J. Appl. Phys. **70**, 2954 (1991).
[6]F. Bozso and Ph. Avouris, Phys. Rev. B **44**, 9129 (1991).
[7]J. T. Yates, Jr., J. Phys. Condens. Matter **3**, S143 (1991).
[8]S. Tanaka, M. Onchi, and M. Nishjima, Surf. Sci. **191**, L756 (1987).
[9]M. Fujisawa, Y. Taguchi, Y. Kuwahara, M. Onchi, and M. Nishijima, Phys. Rev. B **39**, 12 918 (1989).
[10]Y. Taguchi, M. Fujisawa, and M. Nishijima, Chem. Phys. Lett. **178**, 363 (1991).
[11]Y. Taguchi, M. Fujisawa, T. Takaoka, T. Okada, and M. Nishijima, J. Chem. Phys. **95**, 6870 (1991).
[12]See, for example, R. G. Pearson, Inorg. Chem. **27**, 734 (1988).
[13]H. Ibach and D. L. Mills, *Electron Energy Loss Spectroscopy and Surface Vibrations* (Academic, New York, 1982), Chap. 3.
[14]B. N. J. Persson and J. E. Demuth, Phys. Rev. B **30**, 5968 (1984).
[15]B. N. J. Persson, J. G. Ping, Y. B. Xu, D. Frankel, Y. Chen, and G. J. Lapeyre, Phys. Rev. B **40**, 7819 (1989).
[16]P. J. Chen, M. L. Colaianni, and J. T. Yates, Jr., J. Appl. Phys. **72**, 3155 (1992).
[17]W. E. Keller and H. L. Johnston, J. Chem. Phys. **20**, 1749 (1952).
[18]M. Nishijima, K. Edamoto, Y. Kubota, S. Tanaka, and M. Onchi, J. Chem. Phys. **84**, 6458 (1986).
[19]J. E. Northrup, Phys. Rev. B **39**, 1434 (1989).
[20]W. Daum, H. Ibach, and J. E. Müller, Phys. Rev. Lett. **59**, 1593 (1987).
[21]G. S. Glander, P. Akavoor, and L. L. Kesmodel, Phys. Rev. B **44**, 5893 (1991).
[22]J. E. Rowe, R. A. Malic, E. E. Chaban, R. L. Headrick, and L. C. Feldman, J. Electron Spectrosc. Relat. Phenom. **54/55**, 1115 (1990).
[23]H. H. Weitering, J. Chen, N. J. DiNardo, and E. W. Plummer, Phys. Rev. B **48**, 8119 (1993).
[24]H. Ibach, *Electron Energy Loss Spectrometers* (Springer-Verlag, Berlin, 1991), Chap. 7.
[25]A. Borghesi, P. Bottazzi, G. Guizzetti, L. Nosenzo, A. Stella, S. U. Campisano, E. Rimini, F. Cembali, and M. Servidori, Phys. Rev. B **36**, 9563 (1987).
[26]S. M. Sze, *Semiconductor Devices* (Wiley, New York, 1985).
[27]G. L. Pearson and J. Bardeen, Phys. Rev. **75**, 865 (1949).
[28]J. L. Gland, B. A. Sexton, and G. E. Mitchell, Surf. Sci. **115**, 623 (1982).
[29]P. A. Redhead, Vacuum **12**, 203 (1962).
[30]T. Shimanouchi, *Tables of Molecular Vibrational Frequencies*, Natl. Bur. Stand. Ref. Data Ser., Natl. Bur. Stand. (U.S.) Circ. No. 39 (U.S. GPO, Washington, D.C., 1972), Vol. 1.
[31]O. S. Binbrek and A. Anderson, Chem. Phys. Lett. **15**, 421 (1972).
[32]K. Nakamoto, *Infrared and Raman Spectra of Inorganic and Coordination Compounds* (Wiley, New York, 1978), pp. 197–202, and references cited therein.
[33]S.-T. Li, S. Hasegawa, S. Nakamura, and H. Nakashima, Jpn. J. Appl. Phys. **30**, L1671 (1991).
[34]Ph. Avouris and R. Wolkow, Phys. Rev. B **39**, 5091 (1989).
[35]P. Jakob and D. Menzel, Surf. Sci. **220**, 70 (1989).
[36]J. A. Polta and P. A. Thiel, J. Am. Chem. Soc. **108**, 7560 (1986).
[37]G. Herzberg, *Infrared and Raman Spectrum of Polyatomic Molecules* (Van Nostrand, New York, 1945).
[38]Ph. Avouris and J. E. Demuth, J. Chem. Phys. **75**, 4783 (1981).
[39]J. L. Jensen, Prog. Phys. Org. Chem. **12**, 189 (1976).
[40]K. Higashiyama, S. Yamazaki, H. Ohnuki, and H. Fukutani, Solid State Commun. **87**, 455 (1993).
[41]T. M. Grehk, L. S. O. Johansson, U. O. Karlsson, and A. S. Flodström, Phys. Rev. B **47**, 13 887 (1993).